Bond Strength of Lap-Spliced Bars in Concrete Confined with Composite Jackets

D. A. Bournas[1] and T. C. Triantafillou, M.ASCE[2]

Abstract: The effectiveness of fiber-reinforced polymer (FRP) and textile-reinforced mortar (TRM) jackets was investigated experimentally and analytically in this study to confine old-type reinforced concrete (RC) columns with limited capacity because of bond failure at lap-splice regions. The local bond strength between lap-spliced bars and concrete was measured experimentally along the lap-splice region of six full-scale RC columns subjected to cyclic uniaxial flexure under constant axial load. The bond strength of the two column specimens tested without retrofitting was found to be in good agreement with the predictions given by two existing bond models. These models were modified to account for the contribution of composite material jacketing to the bond resistance between lap-spliced bars and concrete. The effectiveness of FRP and TRM jackets against splitting at lap splices was quantified as a function of jacket properties and geometry as well as in terms of the jacket effective strain, which was found to depend on the ratio of lap-splice length to bar diameter. Consequently, simple equations for calculating the bond strength of lap splices in members confined with composite materials (FRP or TRM) are proposed. **DOI: 10.1061/(ASCE)CC.1943-5614.0000078.**

CE Database subject headings: Bars; Bonding; Confinement; Fiber reinforced polymer; Reinforced concrete; Seismic effects; Rehabilitation; Slip; Mortars.

Author keywords: Bond strength; Confinement; FRP; Lap splices; Reinforced concrete; Seismic retrofitting; Slip; Textile-reinforced mortar.

Introduction and Background

Most concrete structures in the seismic regions of the world were constructed before enforcement of modern seismic design codes and are, thus, inherently vulnerable to earthquakes. A significant inadequacy of existing concrete members lies in the mechanism of the bond between longitudinal reinforcement and concrete. Bond-critical regions in concrete structures are, for example, at the base of bridge piers, where the reinforcement is lap spliced with starter bars projecting above the foundation, and the junction between the floor slabs or beams and the columns in reinforced concrete (RC) buildings, where the column reinforcement of two consecutive stories is lap spliced for ease of construction. However, according to modern seismic design philosophy, these locations are where the formation of plastic hinges is expected. To make matters worse, typical old-type RC columns include both short lap splices and low amounts of transverse reinforcement. As a consequence, the bond capacity of lap-spliced bars is often the weak link; remedying it is essential for seismic upgrading of old concrete buildings.

The upgrading of existing RC columns through jacketing has become a popular technique in an increasingly large number of rehabilitation projects. The use of FRPs has gained considerable popularity among all jacketing techniques because of the favorable properties offered by these materials, namely, high strength-to-weight ratio, corrosion resistance, ease and speed of application, and minimal change of geometry. The improved behavior in FRP-confined lap-spliced regions has been demonstrated in many studies (e.g., Saadatmanesh et al. 1997a; Seible et al. 1997; Ma and Xiao 1999; Osada et al. 1999; Ma et al. 2000; Chang et al. 2001; Haroun et al. 2001; Saatcioglu and Elnabelsy 2001; Harries et al. 2006; Brena and Schlick 2007). FRP jackets in regions with straight lap-spliced rebars provide confinement, which increases the friction between lap splices and prevents slippage. This is not of concern in lap splices of smooth (plain) bars with 180° hooks because slippage is not activated (Bousias et al. 2007).

The mechanism by which confinement with FRP jackets contributes to the enhancement of the bond strength between lap-spliced bars in tension and concrete has been investigated in a limited number of studies. Harajli (2005) modified the Orangun equation (Orangun et al. 1977) and proposed a relationship for evaluating the thickness of the FRP jacket required for developing a desired steel stress at the lap-splice bond failure. In another study, Hamad and Rteil (2006), based on experimental data of tension lap splices confined with FRP sheets in normal- and high-strength concrete specimens, proposed a new FRP confinement parameter, which accounts for the increase in bond strength owing to the presence of FRP sheets. However, in both expressions proposed by Harajli (2005) and Hamad and Rteil (2006), the calculated lap-splice bond strength of FRP-confined members depends exclusively on the mechanical characteristics of the jacket, irrespective of the lap splice geometric characteristics (lap length, bar diameter).

In the present study the authors go one step further by investigating experimentally and analytically the use of jackets made of composite materials as a means of enhancing the (poor) bond resistance of lap splices, with a focus on understanding the role of the jacket as a confining element. Those jackets comprise

[1]Postdoctoral Researcher, European Laboratory for Structural Assessment, IPSC, JRC, T.P. 480, I-21020 Ispra (VA), Italy. E-mail: dionysis.bournas@jrc.ec.europa.eu

[2]Professor, Dept. of Civil Engineering, Univ. of Patras, Patras GR-26500, Greece. E-mail: ttriant@upatras.gr

Note. This manuscript was submitted on October 8, 2009; approved on March 18, 2010; published online on April 6, 2011. Discussion period open until September 1, 2011; separate discussions must be submitted for individual papers. This paper is part of the ***Journal of Composites for Construction***, Vol. 15, No. 2, April 1, 2011. ©ASCE, ISSN 1090-0268/2011/2-156–167/$25.00.

either FRP or the new class of inorganic matrix composites, termed textile-reinforced mortars (TRM) (Triantafillou et al. 2006; Triantafillou and Papanicolaou 2006; Bournas et al. 2007, 2009), to enhance the (poor) bond resistance of lap splices. The local bond strength between lap-spliced bars and concrete is measured experimentally at the plastic hinge region (floor level) of large-scale RC columns subjected to simulated seismic loading. In this way, the contribution of FRP or TRM confinement as a means of improving the bond resistance of straight lap splices with deformed bars is assessed. Moreover, two existing analytical bond models are modified to account for the contribution of composite jackets to confinement. In addition, the effectiveness of FRP or TRM jackets against splitting at lap splices is quantified as a function of jacket properties and geometry and in terms of the jacket effective strain, which depends on the ratio of lap splice length to bar diameter. Finally, this study proposes simple models for calculating the bond strength of lap splices in members confined with FRP or TRM jackets.

Experimental Program

Test Specimens and Experimental Parameters

Seven full-scale reinforced concrete column specimens with the same geometry, six with lap splicing of longitudinal bars at the floor level and one with continuous longitudinal reinforcement, were constructed and tested under lateral load (Fig. 1). The specimens were flexure-dominated cantilevers with a height to the point of application of the load (shear span) of 1.6 m (half a typical story height) and a cross section of 250×250 mm. The columns were fixed into a heavily reinforced 0.5-m-deep base block, 1.2×0.5 m in plan, within which the longitudinal bars were anchored with 90° hooks at the bottom. To represent old-type nonseismically designed and detailed columns, all specimens were reinforced longitudinally with four 14-mm-diameter deformed bars with an effective depth of 225 mm and 8-mm-diameter smooth stirrups at a spacing of 200 mm, closed with 90° hooks at both ends. Together with the deficient reinforcing details, the concrete cover of the spliced bars in the column section was chosen to a constant low value of 10 mm (hence the ratio of cover to bar diameter $c/d_b = 0.7$), which, especially for short lap splices, would induce splitting bond failures prior to yielding of longitudinal steel bars (e.g., fib 2000). The geometry of a typical cross section is shown in Fig. 1(b).

The effectiveness of FRP or TRM jackets applied at the ends of old-type RC columns was evaluated for two different lap lengths, which were selected equal to 20 and 40 bar diameters, as shown in Fig. 1(b). Columns with the shorter lap lengths (Series L20d_…) are more representative of RC construction up to the late 1970s. These columns were designed as follows: one specimen was tested without retrofitting as control (L20d_C); the second one was retrofitted with a two-layered CFRP jacket (specimen L20d_R2); and the third one was retrofitted with an equal (to its FRP counterpart) stiffness and strength carbon fiber TRM jacket consisting of four layers (specimen L20d_M4). Columns with longer lap lengths (Series L40d_…) are more representative of RC construction up to the late 1990s. These columns were given the notation L40d_C, L40d_R2, and L40d_M4, which except for the lap length, is identical to Series L20d_…. The layers in the TRM-jacketed columns were twice as many compared with their FRP counterparts, resulting in two equivalent confining systems with the same stiffness and strength in the circumferential direction. As explained in the following, the fibers of the two jacketing systems in the circumferential direction were of the same type and nearly twice as many per layer in the FRP system compared with the TRM system.

The jackets extended from the base of each column (a gap of about 10 mm was left) to a height of 430 mm, except for the two columns with longer lap splices (L40d_R2 and L40d_M4) where the jackets were extended to a height of 600 mm. The height of 430 mm was selected to fulfill the requirements for exceeding the theoretical plastic hinge length (as per various models), as well as for practical reasons: this height corresponds to approximately $1/3$ of the total width of the textile used, 1.28 m. In the same way, in the case of columns with longer lap lengths, a height of 600 mm corresponds to approximately one half of the total width of the textile used and exceeds the plastic hinge length and the lap splice length of $40d_b = 560$ mm. The overlapping length of the jacket was 150 mm. Prior to jacketing, the four corners of the columns that received jacketing were rounded at a radius equal to 25 mm. A summary of the experimental parameters and retrofitting schemes is presented in Table 1.

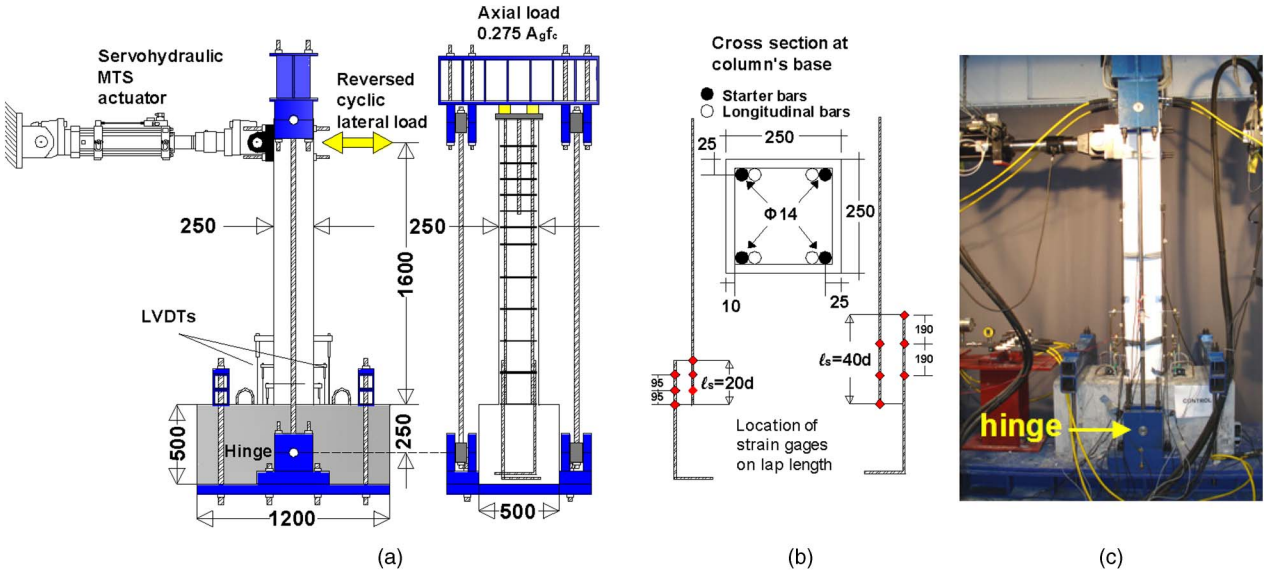

Fig. 1. (a) Schematic of test setup; (b) cross section of the columns and distribution of strain gauges along the lap length; (c) photograph of test setup

Table 1. Experimental Parameters

Specimen notation	Lap length	Concrete strength f_c (MPa)	Confinement with composite materials: Jacketing material	Confinement with composite materials: No. of layers/jacket's height
L0_C	—	28.9	—	—
L20d_C	$20d_b = 280$ mm	27.8	—	—
L20d_R2	$20d_b = 280$ mm	26.5	FRP	2/430 mm
L20d_M4	$20d_b = 280$ mm	26.3	TRM	4/430 mm
L40d_C	$40d_b = 560$ mm	25.8	—	—
L40d_R2	$40d_b = 560$ mm	25.5	FRP	2/600 mm
L40d_M4	$40d_b = 560$ mm	25.3	TRM	4/600 mm

Materials and Strengthening Procedures

The longitudinal bars had a yield stress of 523 MPa, a tensile strength of 624 MPa, and an ultimate strain of 12% (average values from six specimens). The corresponding values for the steel used for stirrups were 351 MPa, 444 MPa, and 19.5%, respectively. To simulate field conditions, the base blocks and the columns were cast with separate batches of ready-mix concrete (on two consecutive days). Casting of the columns was made with separate batches too, because of the unavailability of a large number of molds. The compressive strengths on the day of testing the columns (average values from three specimens) are presented in Table 1 for all columns. The average compressive strength and standard deviation were 26.59 MPa and 1.31 MPa, respectively, suggesting that the variability in concrete strength would not significantly affect the column test results. Cylinders with a diameter of 150 mm and a height of 300 mm were also used to obtain the splitting tensile strength of the concrete; the average tensile strength which was obtained from six specimens with lap-spliced bars on the day of testing the columns was 3 MPa.

For the specimens receiving FRP jacketing, L20d_R2 and L40d_R2, a commercial unidirectional carbon fiber sheet with a weight of 300 g/m^2 and a nominal thickness of 0.17 mm, was used. The mean tensile strength and elastic modulus of the carbon fibers was taken from data sheets with 3,800 MPa and 230 GPa, respectively. For the specimens receiving TRM jacketing, L20d_M4 and L40d_M4, a commercial textile with an equal quantity of high strength carbon rovings in two orthogonal directions, was used. Each fiber roving was 3 mm wide and the clear spacing between rovings was 7 mm. The weight of carbon fibers in the textile was 348 g/m^2 and the nominal thickness of each layer (based on the equivalent smeared distribution of fibers) was 0.095 mm. The mean tensile strength and elastic modulus of the carbon fibers (as well as of the textile, when the nominal thickness is used) was taken from data sheets of 3,800 MPa and 225 GPa, respectively. For the specimens receiving resin adhesive bonding, a commercial structural adhesive (two-part epoxy resin with a mixing ratio 3:1 by weight) with a tensile strength of 70 MPa and an elastic modulus of 3.2 GPa (cured for 7 days at 23°C) was used (properties were provided by the manufacturer). Because the adhesive had low viscosity, complete wetting of the sheets was possible by using a plastic roller. For the specimens receiving mortar as a binding material, a commercial inorganic dry binder was used, consisting of cement and polymers at a ratio of about 8:1 by weight. The water-binder ratio in the mortar was 0.23:1 by weight, resulting in plastic consistency and good workability.

The mortar was applied in approximately 2-mm-thick layers with a smooth metal trowel (the thickness was checked with a magnifying glass after strengthening was completed). After application of the first mortar layer on the (dampened) concrete surface, the textile was applied and pressed slightly into the mortar, which protruded through all the perforations between fiber rovings. The next mortar layer covered the textile completely, and the operation was repeated until all textile layers were applied and covered by the mortar. Of crucial importance in this method, as in the case of epoxy resins, was the application of each mortar layer while the previous one was still in a fresh state.

The strength of mortar used in this study was obtained through flexural and compression testing according to EN 1015-11 (1993), using a servohydraulic MTS testing machine. Flexural testing was carried out on three $40 \times 40 \times 160$ mm hardened mortar prisms, at an age of 28 days. The prisms were prepared and cured in the laboratory until testing, in conditions identical to those for the jackets used for confinement (except for the first two days, when the prisms were inside the molds). The prisms were subjected to 3-point bending at a span of 100 mm and the flexural strength was calculated from the peak load. Compression testing was carried out on each of the fractured parts using two 40×40 mm bearing steel platens on top and bottom of each specimen. The average flexural and compressive strength values were 6.51 MPa and 20.8 MPa, respectively.

Experimental Setup and Procedure

To simulate seismic excitation, the columns were subjected to lateral cyclic loading that consisted of successive cycles progressively increasing by 5 mm of displacement amplitudes in each direction. The loading rate was in the range from 0.2 mm/s to 1.1 mm/s, the higher rate corresponding to higher displacement amplitude, all in displacement-control mode. At the same time, a constant axial compressive load was applied to the columns, corresponding to 27.5% of the members' compressive strength (depending on concrete strength, this load ranged from 435 kN to 496 kN). The lateral load was applied using a horizontally positioned 250 kN MTS actuator and the axial load was exerted by a set of four hydraulic cylinders with automated pressure self-adjustment, acting against two vertical rods connected to the strong floor of the testing frame through a hinge [Figs. 1(a) and 1(c)]. With this setup the P-Δ moment at the base section of the column is equal to the axial load times the tip displacement (i.e., at piston fixing position) of the column times the ratio of hinge distance from the base (0.25 m) and the top ($0.25 + 1.60 = 1.85$ m) of the column (i.e., times $0.25/1.85 = 0.135$).

Displacements and rotations at the plastic hinge region were monitored using six rectilinear displacement transducers (three on each side, perpendicular to the piston axis) fixed at cross sections 1, 2, and 3, with a distance of $\ell_1 = 130$ mm; $\ell_2 = 260$ mm; and $\ell_3 = 450$ mm, respectively, from the column base, as shown in Fig. 1(a). The instrumentation also consisted of a total of 12 strain gauges for each column with lap splices, which were mounted on one pair of lapped bars (starter-longitudinal) per column side as follows [Fig. 1(b)]: (a) three along the starter bars, at distances from the column base of 0, 95, and 190 mm for Series L20d_…, or 0, 195, and 390 mm for Series L40d_…; and (b) three along the longitudinal bars, at distances from the column base of 95, 190, and 280 mm for Series L20d_…, or 195, 390, and 560 mm for Series L40d_…. Measurements from the strain gauges on each pair of starter-longitudinal bars were used to determine the strain distribution of bars and bond stresses along the splice length.

Test Results and Discussion

Detailed results in terms of load-displacement hysteresis loops, curvature, and energy dissipation are given in Bournas et al. (2009).

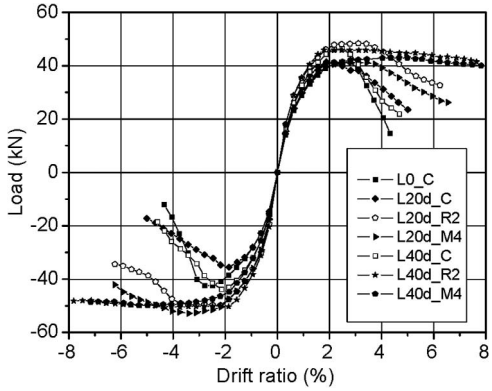

Fig. 2. Load versus drift ratio envelope curves

In this paper, the authors present only those (additional) test results related to bond strength at lap splices. The response of all columns tested is given in Fig. 2 in the form of load-drift ratio (obtained by dividing the tip deflection by the specimen's height) envelope curves. Key results are also presented in Table 2, which includes (a) the peak resistance in the two directions of loading; (b) the ratio of the starter bars (projecting from the foundation) steel stress f_{sL}, developed at the columns' peak resistance, over their yield stress f_{yL} in the two directions of loading. The starter bars steel stresses were calculated from the corresponding measured steel strains at the region of maximum moment, by assuming a bilinear stress-strain relationship; (c) the average bond strength (corresponding to peak resistance) τ_{av}, developed over the splice length in the two directions of loading; (d) the ratio of average bond strength (corresponding to peak resistance) τ_{av}, over the square root of the concrete's compressive strength f_c. In most descriptive and design expressions, as long as the concrete strength remains below approximately 55 MPa, the effect of concrete properties on bond strength is represented adequately by using the square root of the compressive strength; (e) the total slip of spliced bars over the splice length (as explained below, equal to the fixed-end slip at the column—footing interface) at conventional failure of the column, defined as reduction of peak resistance in a cycle below 80% of the maximum recorded resistance in that direction of loading; and (f) the observed failure mode.

The performance and failure mode of all tested specimens with lap splices was controlled by flexure. The failure mode of the unretrofitted specimen with continuous longitudinal bars L0_C was controlled by buckling of longitudinal rebars above the column base [Fig. 3(a)], which led to direct lateral strength degradation. Both unretrofitted specimens with lap splices (L20d_C and L40d_C) experienced splitting bond failure. More specifically, significant longitudinal and horizontal splitting cracks developed along the splice length of lapped bars for both unretrofitted specimens L20d_C [Fig. 3(b)] and L40d_C [Fig. 3(c)] at drift ratios of 1.56% and 2.5%, respectively, corresponding to peak lateral load. The length and width of the longitudinal cracks along the splice length was increasing at higher drift levels as the bond between reinforcing bars and concrete was deteriorating. As a result, the concrete under compression spalled [Fig. 3(d)] along the lower 100 mm and 175 mm (approximately) from the base of specimens L20d_C and L40d_C, respectively, leading to substantial lateral strength degradation after peak lateral load.

Contrary to the control specimen L0_C with continuous bars, in unretrofitted specimens with lap splices the expansive spalling of the concrete in the critical zone was not followed by buckling of longitudinal rebars for two reasons: first, the compression reinforcement was doubled; second, the quick strength degradation of the specimens associated with the extensive bond deterioration (described in next sections) reduced the demand of the compression reinforcement to resist the applied load. The drift ratio at failure (average values for both loading directions) sustained by unretrofitted columns L20d_C and L40d_C was 3.59% and 3.28%, respectively.

Finally, the lap-spliced specimen L40d_C showed a slightly higher resistance, when compared with the control specimen L0_C. This difference may be considered within the range of experimental scatter or may be attributed to the fact that compression reinforcement was doubled in specimen L40d_C.

FRP- and TRM-jacketed columns, with either short or long lap length, responded far better than their unretrofitted counterparts both in terms of strength and deformation capacity at failure. Confinement provided the columns with sufficient resistance

Table 2. Summary of Test Results

	Peak force (kN)		Steel stress at peak force f_{sL}/f_{yL}		Bond strength τ_{av} (MPa)		$\tau_{av}/\sqrt{f_c}$		Slip at "failure" (mm)		
Specimen notation	Push	Pull	Push	Pull	Push	Pull	Push	Pull	Push	Pull	Failure Mode
L0_C	41.63	−42.48	1	1	—	—	—	—	—	—	Buckling of longitudinal bars
L20d_C	41.50	−36.62	0.83	0.66	4.42	—	0.83	—	5.6	3.1	Splitting bond failure followed by spalling of the concrete cover
L20d_R2	41.26	−52.86	0.95	1	6.78	6.86	1.32	1.34	13.4	10.8	Splitting longitudinal cracking followed by pull-out bond failure of lapped bars
L20d_M4	48.46	−49.80	1	1	6.03	6.82	1.17	1.33	10.9	6.5	Splitting longitudinal cracking followed by pull-out bond failure of lapped bars
L40d_C	46.26	−43.87	1	0.83	2.95	2.03	0.58	0.40	6.4	6.7	Splitting bond failure followed by spalling of the concrete cover
L40d_R2	42.97	−49.80	1	1	3.06	3.05	0.60	0.60	19.0	20.0	Conventional failure was not reached
L40d_M4	45.90	−50.48	1	1	—	2.93	0.58	0.61	21.3	19.9	Conventional failure was not reached

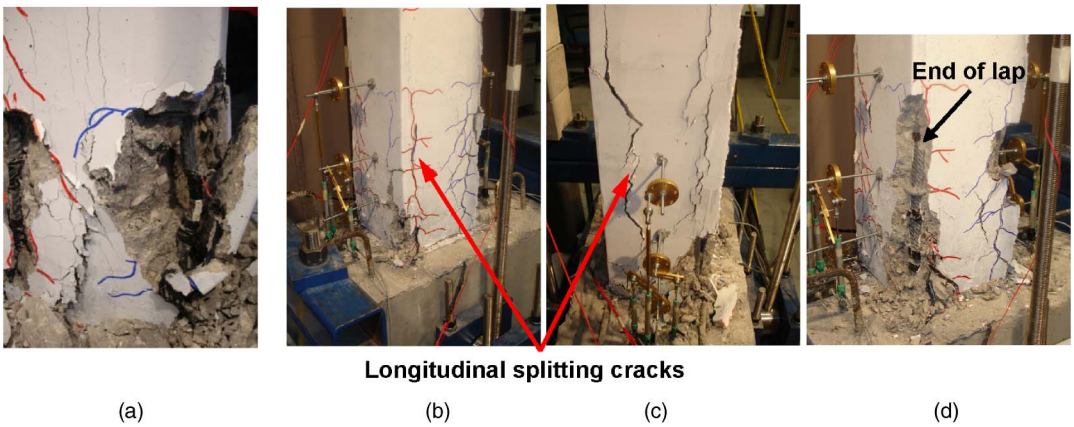

Fig. 3. (a) Disintegration of concrete and bar buckling; longitudinal splitting cracks for specimens; (b) L20d_C; (c) L40d_C; (d) failure of unretrofitted column L20d_C

against splitting cracks and lateral expansion of concrete. Thus, spalling of the concrete cover was controlled and the slip along the splice length was progressively increased in proportion to the horizontal displacement without significant bond stress deterioration.

For both FRP- and TRM-confining systems, the effectiveness of confinement was limited to 20 bar diameters for short lap length compared with 40 bar diameters for long lap length. Specimens L20d_R2 and L20d_M4 (with short lap lengths) sustained reversed deformation cycles up to 6.3% drift before failing because of pull-out bond failure of the spliced bars at an average bond strength (in both directions of loading) between lap-spliced bars and concrete of 6.8 MPa and 6.4 MPa, respectively. Pull-out bond failure occurred when longitudinal splitting cracks had propagated along the entire splice length; thus at that point, the presence of FRP or TRM jacket had no effect on the residual splice capacity. Finally, in specimens L40d_R2 and L40d_M4 where the calculated bond stresses were much lower, 3.1 MPa and 2.9 MPa, respectively, bond failures and spalling of concrete were suppressed until the end of the test at a drift ratio of 7.81%.

For columns L20d_R2 and L20d_M4, the mean strength increase (in both directions of loading) for both confining systems was 20.3% and 25.6%, respectively, in comparison with the control specimen (L20d_C), while the corresponding increase in deformation capacity was 64.7% and 38.8%, respectively. Columns with longer lap splices (L40d_R2 and L40d_M4) behaved in an identical manner until the end of the test at a drift ratio of 7.81% (maximum stroke of piston was reached), resulting in an increase of the members' deformation capacity by a factor of more than 2.5. Peak resistance was practically the same as in the unretrofitted column, indicating that a lap splice length of 40 diameters is adequate for the development of the columns' full strength.

Lap Splice Bond Strength

Steel Strain Histories and Evaluation of Bond Strength over the Splice Length

Fig. 4 illustrates typical strain histories of starter spliced bars at the cross section of maximum moment (column's base). According to the measured steel strains and by assuming a bilinear (elastic-perfectly plastic) stress-strain constitutive law for the steel, the force developed on spliced bars can be estimated. Hence, based on the calculated steel stresses corresponding to peak lateral force (ratio f_{sL}/f_{yL} in Table 2), a lap splice length of 20 bar diameters is

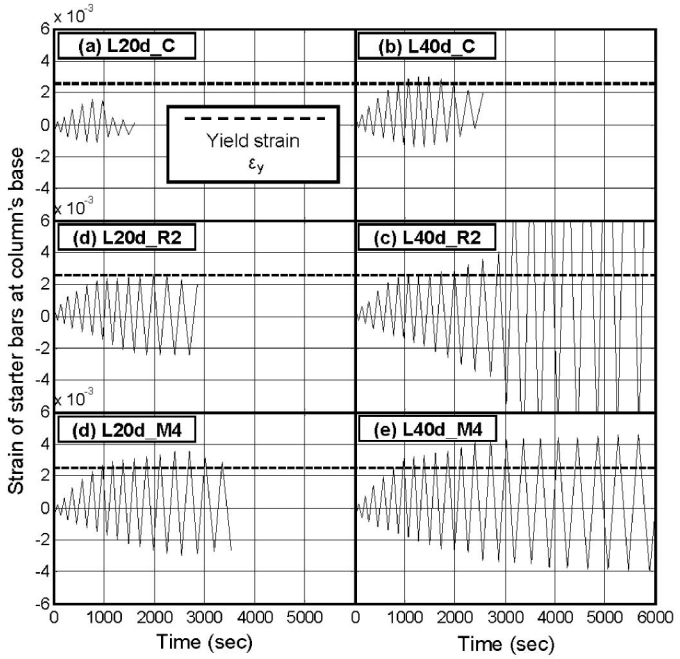

Fig. 4. Typical steel strain histories of starter bars at the column base

not adequate for the development of the longitudinal bars' yield stress. The longer lap length of 40 bar diameters was found to be sufficient for the development of yielding in the push direction only, a fact which is consistent with the slightly higher strength of specimen L40d_C in this direction. The steel strain distribution along the splice length is also useful to evaluate the force transfer between longitudinal and starter bars into the base block and to determine the local bond stress in the lap splice region.

The bond stress (τ) distribution between spliced bars and the surrounding concrete was calculated using the discrete strain readings [Fig. 5(a)] along the splice length, as follows:

$$\tau_i = (d_b E_s/4)(\Delta\varepsilon/\Delta x) = (d_b E_s/4)[(\varepsilon_i - \varepsilon_{\iota-1})/(x_i - x_{i-1})] \quad (1)$$

where d_b = diameter of lapped bars; E_s = modulus of elasticity of steel; ε_i = axial strain of starter and longitudinal bars at discrete locations of strain gauges; and x = coordinate along the splice length. The x axis starts from the free end of the starter and longitudinal bars, respectively, as shown in Fig. 5(a).

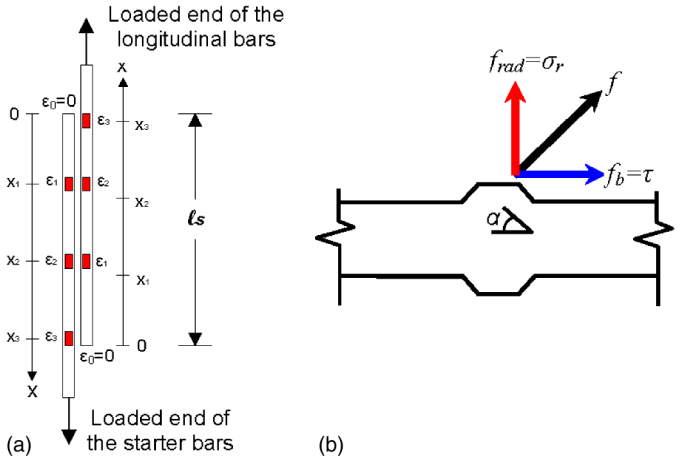

Fig. 5. (a) Position of the strain gauges and symbols used in bond analysis; (b) bond and radial stresses developed at lugs

Based on Eq. (1) and by assuming zero strain at the free ends of spliced bars, the bond strength distribution along the splice length, corresponding to peak lateral force, was computed. Fig. 6 shows this distribution for both starter and longitudinal bars (left-hand and right-hand side, respectively) in each direction of loading, and provides the average bond strength along the lap splice (mean value for both directions of loading). By comparing the average bond strength of confined specimens, confinement was much more effective in terms of bond strength enhancement in the case of the shorter lap length. Additionally, FRP jackets were found to be slightly more effective in terms of bond strength enhancement compared with TRM jackets of equal stiffness and strength.

The oblique bearing force exerted by the lugs of a bar [Fig. 5(b)] against bar pull-out is higher in the case of the shorter lap splices (Series L20d_…) because the number of lugs participated over the splice length is smaller when compared with the longer lap splices (Series L40d_…). Thus, the longitudinal component of this bearing force, which results in what is defined as bond stress (τ), is much higher for the columns with the lap length of 20 bar diameters, as confirmed in Fig. 6. Correspondingly, the transverse component of this bearing force creates a radial stress (σ_r) that is responsible for splitting the surrounding concrete; this radial stress is also higher for the shorter lap length, especially near the lap splice ends. Steel plants worldwide construct deformed reinforcing bars with a rib angle α [Fig. 5(b)] of about 45°; consequently the two components of bond forces are approximately equal. Therefore, the bond stress distribution presented in Fig. 6 is almost the same as the distribution of radial stresses (causing concrete splitting) along the lap splice length.

Overall, for columns with short lap lengths (L20d_R2 and L20d_M4) the increase in bond strength (and, approximately, in the radial stress, σ_r) for the two confining systems with FRP and TRM jackets was equal to 54% and 45%, respectively. The corresponding increases for the specimens with long lap splices (L40d_R2 and L40d_M4) were 23% and 18%, respectively.

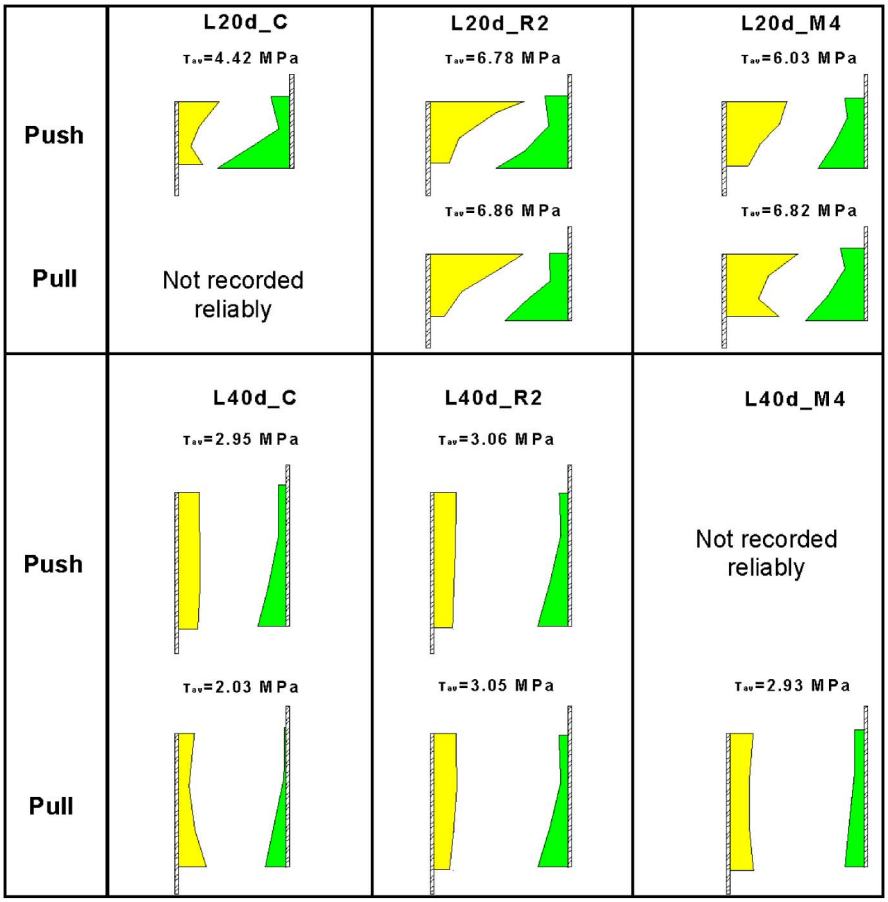

Fig. 6. Bond stress distribution between spliced bars and concrete along the lap length and average bond strength of the lap splice in each direction of loading; starter bars are shown on the left

Analytical Bond Models for Lap Splices

The main parameters that influence the bond capacity between concrete and spliced bars in tension include the concrete cover, the splice length, the compressive strength of concrete, the bar diameter, the reinforcing bar geometry, and concrete confinement.

Zuo and Darwin (2000), based on a database with 171 specimens containing bars not confined by transverse reinforcement and 196 specimens containing bars confined by transverse reinforcement, proposed a statistically based expression for calculating the lap splice bond strength $\tau_{\max}$. This formulation incorporates the effects of coarse aggregate quantity and type and rebar geometry. This expression forms the basis for the bond recommendations of ACI Committee 408 (2003). The Zuo and Darwin (2000) expression is given as follows:

$$\tau_{\max} = (1/\pi d_b \ell_s)\{[1.44\ell_s(c_{\min} + 0.5d_b) + 56.3A_b][(0.1)(c_{\max}/c_{\min}) + 0.9]f_c^{1/4} + K_{tr,s} \cdot f_c^{3/4}\} \quad (2)$$

where f_c = compressive strength of concrete (MPa); $c_{\min}$ and $c_{\max}$ = minimum and maximum values of concrete cover, respectively; $c_{\min} = \min(c_{so}, c_b, c_{si} + d_b/2)$, $c_{\max} = \max(c_{so}, c_b)$, and the variables c_{so}, c_b, c_{si} are as defined in Fig. 7(a); ℓ_s= splice length; A_b = area of longitudinal bars; and $K_{tr,s}$ = term representing the effect of confinement by steel stirrups, as follows:

$$K_{tr,s} = k_s(Ns_h)(A_{sw}/s_h) + 743.6 = 0.354 t_r t_d/n_s[(Ns_h)(A_{sw}/s_h)] + 743.6 \quad (3)$$

where $t_r = 9.6R_r + 0.28$ = term representing the effect of relative rib area; R_r = ratio of projected rib area normal to bar axis to product of nominal bar perimeter and center-to-center rib spacing; $t_d(mm) = 0.78d_b + 5.6$ = term representing the effect of bar size; s_h = spacing of stirrups; A_{sw} = area of transverse steel reinforcement parallel to the direction of loading, namely, the area of each stirrup or tie crossing potential plane of splitting adjacent to the reinforcement being spliced; f_{yw}= yield stress of stirrups; n_s= number of bars being spliced along plane of splitting; N = number of transverse reinforcing stirrups or ties crossing ℓ_s.

More recently, Lettow and Eligehausen (2006) presented a semiempirical expression, Eq. (4), for calculating the maximum stress f_{sm} that can be developed by the tensile bars in lap splice regions of the splitting bond failure

$$f_{sm} = 24.2(\ell_s/d_b)^{0.55}(f_c)^{1/4}(c_d/d_b)^{1/3} \times (c_{\max}/d_b)^{0.1}(20/d_b)^{0.2}(1 + K_{tr,s}) \quad (4)$$

where $c_d = \min(c_{so}, c_b, c_{si})$ and $c_{\max} = \max(c_{so}, c_b, c_{si})$. This equation has been based on an extended database of 793 test results including 402 specimens without transverse reinforcement and 391 specimens with transverse reinforcement, for which a quite good agreement with the experimentally measured steel stresses exists (the mean value of the experimental to analytical ratio is equal to 1.0 with a variation of 15%). Eq. (4), which will also be used in the new Model Code of *fib* (possibly in a slightly revised form), can be applied for the calculation of the bond strength between lap-spliced bars and concrete, as follows:

$$\tau_{\max} = (d_b/4\ell_s)[24.2(4\ell_s/d_b)^{0.55}(f_c)^{1/4}(c_d/d_b)^{1/3} \times (c_{\max}/d_b)^{0.1}(20/d_b)^{0.2}(1 + K_{tr,s})] \quad (5)$$

$$K_{tr,s} = k_s(A_{sw}n_{l,sw}/s_h) = (10/d_b n_s)(A_{sw}n_{l,sw}/s_h) \quad (6)$$

where $n_{l,sw}$ = number of transverse reinforcing bar legs (stirrups or ties) crossing splitting cracks as defined in Fig. 7(a). The preceding equations has the following limitations: $20/d_b \le 1.0$; $1.0 \le c_d/d_b \le 3.0$; $c_{\max}/c_{\min} \le 5.0$; and $10K_{tr,s} \le 0.4$.

The predictions of Eqs. (2) and (5) were compared with the experimentally measured bond strengths at the lap splice region of the two unretrofitted specimens L20d_C and L40d_C. In the case of the shorter lap length, the prediction-to-test ratios were 0.92 and 0.96 for Eqs. (2) and (5), respectively. The agreement between the analytical prediction of Zuo and Darwin's (2000) model and the experimental value was quite good, while the best match was obtained with Lettow and Eligehausen's (2006) model. For the longer lap splice of 40 bar diameters, the prediction-to-test ratios were 1.08 and 1.22 for Eqs. (2) and (5), respectively. Here, the best match was obtained for Zuo and Darwin's (2000) model.

Overall, it may be concluded that the predicted bond strengths according to Zuo and Darwin's (2000) and Lettow and Eligehausen's (2006) models are generally in good agreement with the experimentally measured bond strengths for both lap lengths. For this reason and because these two approaches form the basis of code formulations (ACI 408 Committee and new fib Mode Code), they are modified in the next section to account for the contribution of FRP or TRM confinement on the local bond strength between lap-spliced reinforcing bars and surrounding concrete. However, the approach described in the next section is general and could be applied in the future to other bond strength models.

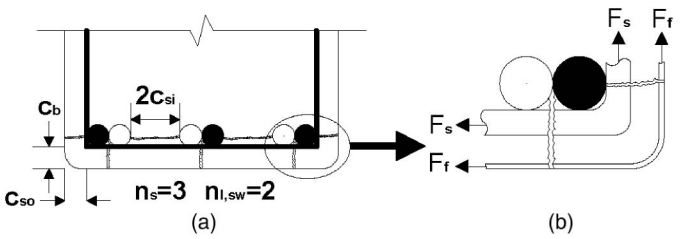

Fig. 7. (a) Definition of c_b, c_{si} and c_{so}; (b) forces induced by stirrups and TRM or FRP jackets against side- and face-splitting cracks

Bond Strength of TRM- and FRP-Confined Concrete

TRM and FRP jackets provide additional to the transverse steel reinforcement tension resistance against splitting cracks, as illustrated in Fig. 7(b). To account for this contribution of FRP or TRM confinement on the local bond strength of lap splices, it is reasonable to add a new parameter $K_{tr,j}$ to the transverse reinforcement parameter $K_{tr,s}$ provided by the stirrups. The proposed modified term $K_{tr,t}$, which accounts for the total confinement applied by both the contribution of stirrups and FRP or TRM jackets, is expressed as

$$K_{tr,t} = K_{tr,s} + K_{tr,j} = [\text{linearfunctionof}(A_{sw}/s_h)] + k_f 2nt_f \quad (7)$$

where k_s = calibration factor for steel transverse reinforcement of each bond model as defined in Eqs. (3) and (6); k_f = calibration factor for the effectiveness of FRP or TRM jackets; n = number of layers of fiber sheet or textile layer; and t_f = thickness of one fiber sheet or textile layer. The proposed factor k_f is given by Eqs. (8*a*) and (8*b*) for both models of Zuo and Darwin (2000) and Lettow and Eligehausen (2006), respectively.

Modified Zuo and Darwin (2000):

$$k_f = k_s h_f (E_f/E_s)(\varepsilon_{f,ef}/\varepsilon_{sw}) \quad (8a)$$

Modified Lettow and Eligehausen (2006):

$$k_f = k_s(E_f/E_s)(\varepsilon_{f,ef}/\varepsilon_{sw}) \quad (8b)$$

where h_f = height of FRP or TRM jacket; E_f = elastic modulus of the jacket in the fiber (circumferential) direction; ε_{sw} = average effective strain of the stirrups in the circumferential direction; and $\varepsilon_{f,ef}$ = average effective strain of the jacket in the fiber direction.

The proposed parameter $K_{tr,j}$ takes into account all the characteristics of the jacket: namely, the area of external FRP or TRM reinforcement ($2nt_f$) in the splice region; the modulus of elasticity of the jacket's material (E_f); and the average effective strain of the jacket in the circumferential direction ($\varepsilon_{f,ef}$). The jacket's height h_f is included only in proposed Eq. (8*a*), as it corresponds to the equivalent term Ns_h of stirrups used in Zuo and Darwin's (2000) model. An upper limit for h_f with respect to the lap length (h_f/ℓ_s), defined by pull-out failure, has to be set, beyond which the increase of the jacket's height will have marginal effect, if any, on the bond capacity of the spliced bars. Based on the current experimental results, the determination of such a limit for h_f is not possible, as the interaction between τ_{max} and the ratio h_f/ℓ_s has not been investigated. On the other hand, application of Eq. (8*b*), based on Lettow and Eligehausen's (2006) approach, for the evaluation of bond strength of RC members confined by FRP or TRM, is based on the assumption that the jacket's height is at least equal to the lap length.

The yield stress of the transverse reinforcement was removed from the two bond models presented previously because it was found to have no effect on the lap-splice bond strength. This effect was not measurable in most of the test results (included in the relevant databases), because splitting bond failures of the lap splice preceded yielding of stirrups. Nevertheless, the percentage of activation of the transverse steel reinforcement in the circumferential direction against splitting cracks, which is quantified by the average effective strain of stirrups ε_{sw}, has to be addressed. In this study, with the purpose of determining ε_{sw}, the authors made a careful interpretation of test results on RC members with lap splices. Of particular importance were those results corresponding to specimens in which strain gauges were affixed on the stirrups crossing the lap length (Cairns and Arthur 1979; Lukose et al. 1982; Paulay 1982; Panahshahi et al. 1992; Valluvan et al. 1993; Saadatmanesh et al. 1997b; Azizinamini et al. 1999; Haroun et al. 1999; Ma and Xiao 1999; Melek and Wallace 2004). The determination of ε_{sw} was carried out for various lap lengths at the lap splice splitting bond failure. In general, the distribution of strains on stirrups over the splice region was nonuniform. Only the two outermost stirrups (loaded ends of starter and longitudinal bars) reached the yield strain at the lap-splice bond failure, while the interior stirrups were strained below their yield strain. Thus, an average (over the lap length) experimental value for the effective strain ε_{sw} of stirrups, corresponding to members' bond failure, was considered for each experimental study; this value is given in Table 3. Despite the variation of bond lengths and of splitting failure modes (side or face) among different researchers, the strains measured on stirrups were quite close, with a standard deviation of 0.0024%. Hence, an average value from all the experimental studies is approximately adopted for ε_{sw}, equal to 0.134%, which is lower than the yielding strain of the stirrups. This is consistent with the fact that the yield stress of stirrups was removed from the two aforementioned bond models.

The only term in the proposed modified bond models that is still to be addressed is the average effective strain of the jacket in the circumferential direction $\varepsilon_{f,ef}$. According to the authors, this value depends on the lap length to bar diameter ratio ℓ_s/d_b. For jacketed columns with short lap splices, the radial stresses induced over the splice length (equal to bond stresses for $\alpha = 45°$) are much higher in comparison with the tensile strength of concrete, especially at the lap splice end (Fig. 6). Thus the splitting bond cracks propagate outside the lap splice region, until the radial stresses degrade below the tensile strength of concrete (3 MPa in the current study), in a length which increases as the initial lap length decreases. For short lap splices, the composite jacket's part that extends outside the lap splice region is activated more than for longer lap splices, because it acts against the propagation of longitudinal splitting cracks in a more extended zone. This mechanism is illustrated in Fig. 8.

According to the experimental results of this study (Table 2), the average bond strength along the splice length was increased by 54% and 23% for FRP-confined specimens, and by 45% and 18% for TRM-confined specimens with respect to their unconfined counterparts, for the lap lengths of 20 and 40 bar diameters, respectively. Based on these increases of the bond strength and by using Eqs. (2)–(8), the average strain in which the composite jackets were activated $\varepsilon_{f,ef}$ was determined indirectly. These average strains of FRP and TRM jackets are presented in Table 4 for the two lap lengths investigated here and for both bond models.

Table 3. Experimentally Measured Strains of Stirrups Placed in Lap Splice Regions

Reference	Specimen type	ε_{sw}	ε_{yw}	$\varepsilon_{sw}/\varepsilon_{yw}$
Cairns and Arthur (1979)	Columns	0.0010	0.0017	0.60
Lukose et al. (1982)	Beams	0.0014	0.0023	0.63
Paulay (1982)	Columns	0.0015	0.0015	1.00
Panahshani et al. (1992)	Beams	0.0011	0.0023	0.48
Valluvan et al. (1993)	Columns	0.0016	0.0024	0.66
Saadatmanesh et al. (1997b)	Columns	0.0010	0.0018	0.55
Azizinamini et al. (1999)	Beams	0.0015	0.0021	0.71
Haroun et al. (1999)	Columns	0.0016	0.0022	0.73
Ma and Xiao (1999)	Columns	0.0015	0.0015	1.00
Melek and Wallace (2004)	Columns	0.0012	0.0024	0.50

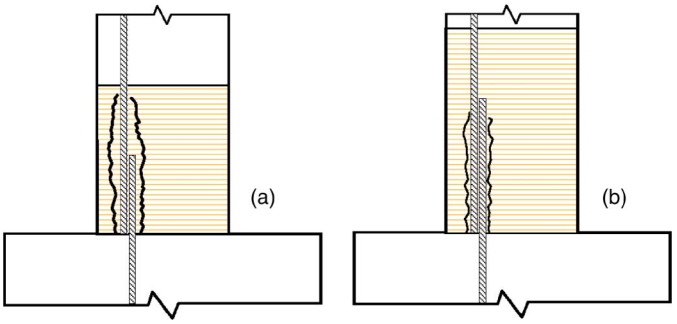

Fig. 8. Activation of FRP or TRM jacket against longitudinal splitting crack propagation in cases of (a) short; (b) long lap splice lengths

Table 4. Average Lateral Effective Strain of FRP and TRM Jackets

	Average lateral effective strain of the jacket, $\varepsilon_{f,ef}$			
	FRP		TRM	
Modified model	$\ell_s = 20d_b$	$\ell_s = 40d_b$	$\ell_s = 20d_b$	$\ell_s = 40d_b$
Zuo and Darwin (2000)	0.0044	0.0019	0.0034	0.0013
Lettow and Eligehausen (2006)	0.0031	0.0013	0.0023	0.0009

The average effective strain of the jacket in the circumferential direction $\varepsilon_{f,ef}$ for different values of lap length to bar diameter, ranging from 15 to 45, as shown in Fig. 9, assuming a linear fit. These diagrams are based on limited test results and on specific values for the stiffness $2nt_fE_f$ of the composite jackets, equal to 156.4 kN/mm and 175 kN/mm for FRP and TRM, respectively. More tests on FRP or TRM confined columns with different lap lengths are necessary to provide the best fit to the preceding diagrams. Moreover, other materials (e.g., glass, basalt) with different modulus of elasticity or jackets with a different number of layers may also result in different values for the effective strain.

Fig. 9 illustrates a high activation (high $\varepsilon_{f,ef}$) of FRP or TRM jackets for short lap lengths that becomes lower as the lap length increases. A key point here is that in the case of short splitting cracks (short lap splices) the activation of the jacket's part outside the lap length ℓ_s is enhanced, a fact quantified by the increased jacket effective strain $\varepsilon_{f,ef}$. In this way, it is possible to estimate the effect of jacket confinement on RC members with lap splices as a function of lap-splice length and jacket stiffness, contrary to current practice, based on the work of Seible et al. (1997), who proposed a fixed value for the circumferential jacket strain corresponding to the onset of splitting in the range 0.001–0.002 (insert in Fig. 9). Using these strains (0.001–0.002) to a jacket design may be quite conservative for low values of ℓ_s/d_b, yielding an unrealistically large number of layers. The equations proposed in this study for the effective strain in an FRP or TRM jacket at lap splice failures are summarized for the two modified models:

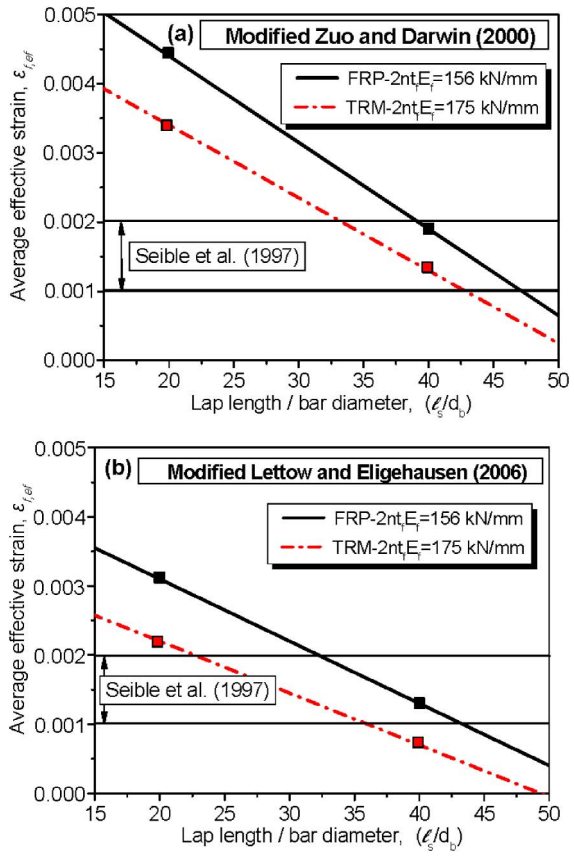

Fig. 9. Diagrams for the evaluation of the average effective strain of FRP or TRM jackets according to (a) the modified Zuo and Darwin (2000) model; (b) the modified Lettow and Eligehausen (2006) model

Modified Zuo and Darwin (2000) model:

$$\varepsilon_{f,ef} = 0.0069–12.5 \cdot 10^{-5}(\ell_s/d_b) \quad \text{for FRP jackets} \tag{9a}$$

$$\varepsilon_{f,ef} = 0.0055–10.5 \cdot 10^{-5}(\ell_s/d_b) \quad \text{for TRM jackets} \tag{9b}$$

Modified Lettow and Eligehausen (2006) model:

$$\varepsilon_{f,ef} = 0.0049–9 \cdot 10^{-5}(\ell_s/d_b) \quad \text{for FRP jackets} \tag{9c}$$

$$\varepsilon_{f,ef} = 0.0037–7.5 \cdot 10^{-5}(\ell_s/d_b) \quad \text{for TRM jackets} \tag{9d}$$

Circumferential FRP strains at the base of rectangular columns with lap splices have actually been measured experimentally by a few researchers, namely Harajli and Dagher (2008) and ElGawady et al. (2010). The former reported a value of 0.00135 for a lap splice length equal to 30 bar diameters; the latter reported values in the range 0.0013–0.0023 for a lap splice length equal to 36 bar diameters. Those independently measured strains are in reasonable agreement with the modified Lettow and Eligehausen (2006) equation, which predicts strains equal to 0.0022 and 0.0017 for the Harajli and Dagher (2008) and the ElGawady et al. (2010) test results, respectively. The comparison with the modified Zuo and Darwin (2000) is less favorable, a fact which adds more confidence to Eqs. (9*c*) and (9*d*) as compared with Eqs. (9*a*) and (9*b*).

Determination of Slip along Lap Splice Length

The global slip over the lap splice length comprises the fixed-end slip at the column-footing interface, the slip attributable to yield penetration into the column footing, the slip attributable to the spliced bars elongation, and the slip attributable to the whole starter bar's pull-out inside the anchorage region. The last one is negligible here, because of the hook restraint located at the starter bars' end into the base block footing, as illustrated in Fig. 10.

The slip resulting from accumulated axial strains in the anchorage region (slip attributable to yield penetration) can be calculated by integrating the bars' strains over the portion of the bar between the interface of maximum axial strain and the point with no axial strain (Sezen and Moehle 2003).

$$s_d = \int_0^{\ell_d} \varepsilon dx = (\varepsilon_{sL}\ell_d/2), \quad \text{for } \varepsilon_{sL} \le \varepsilon_y \tag{10a}$$

$$s_d = \int_0^{\ell_d} \varepsilon dx + \int_{\ell_d}^{\ell_d+\ell_{dy}} \varepsilon dx = (\varepsilon_{sL}\ell_d/2) + (\ell_{dy}/2)(\varepsilon_{sL} + \varepsilon_y),$$
$$\text{for } \varepsilon_s > \varepsilon_y \tag{10b}$$

where s_d = slip attributable to yield penetration of longitudinal bars in the anchorage region; and ℓ_d and ℓ_{dy} = development lengths of the elastic and plastic region of the bars, respectively. In addition,

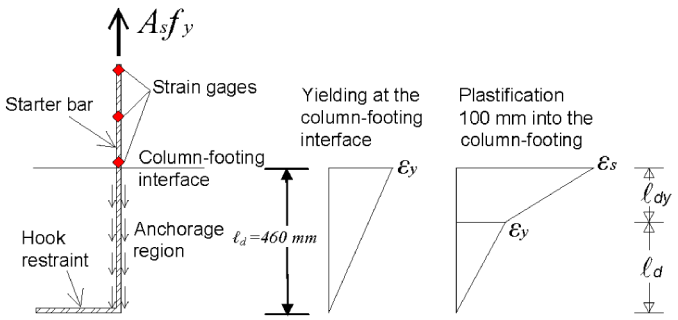

Fig. 10. Slip attributable to yield penetration into the column footing

the slip attributable to the spliced bars' elongation (s_{el}) over the lap splice region can be calculated based on the discrete strain gauge readings [Fig. 5(a)], as follows:

$$s_{el,i} = s_{i-1} + (1/2)(\varepsilon_{i-1} + \varepsilon_i)(x_i - x_{i-1}) \quad (11)$$

Based on the bilinear strain distribution shown in Fig. 10 and Eqs. (10*a*) and (10*b*), the slip attributable to yield penetration in the anchorage region was quantified for two boundary conditions. For the case of unjacketed specimens, where it was considered that longitudinal bars yield only at their loaded end, that is the column-footing interface, this slip was calculated equal to $s_d = 0.60$ mm. In the case of FRP- and TRM-confined specimens, this slip was calculated equal to $s_d = 1.84$ mm, corresponding to a plastification length of starter bars into the column-footing equal to 100 mm ($\ell_{dy} = 100$ mm and $\varepsilon_s = 0.02$). In the absence of strain gauges in the anchorage region of starter bars, their strain distribution was assumed approximately equal to the strain distribution measured by strain gauges at the lap splice region, even though the anchorage length was slightly different from the lap lengths. This assumption was made to provide a qualitative estimation of the contribution of slip attributable to yield penetration of starter bars into the column footing to the global slip.

The fixed-end slip at the column-footing interface is equal to the crack width (w_c) at this interface, which can be calculated as $w_c = \Delta\ell_2 - \varepsilon_{\text{flex}}\ell_2 = \Delta\ell_1 - \varepsilon_{\text{flex}}\ell_{21}$, where $\Delta\ell_1$ and $\Delta\ell_2$ = elongations measured by the displacement transducers cross sections 1 and 2, respectively, (as defined previously, that is at distances $\ell_1 =$ 130 mm and $\ell_2 = 260$ mm from the column base, respectively); and $\varepsilon_{\text{flex}}$ = mean strain in the extreme tension fiber at the column base, equal to $(\Delta\ell_2 - \Delta\ell_1)/(\ell_2 - \ell_1)$. The fixed-end slip at the column-footing interface (attributable to the large opening of a major crack) is a function of horizontal displacement and is independent of external confinement. As a consequence, no significant reduction of slip can be achieved through confinement at joint regions, because the fixed-end slip at the base crack cannot be controlled. Similar observations have been made by Harajli and Rteil (2004). Hence, it is ineffective to provide stiff jackets with the aim to control the fixed-end slip.

The slip attributable to yield penetration into the column-footing was found to vary between 5 and 10% of the fixed-end slip for both unconfined and confined specimens, respectively; while the slip attributable to the spliced bars elongation over the lap splice region was determined approximately equal to 2–3% of the columns' fixed-end slip. For the sake of simplicity, the slip for the calculation of the bond stress-slip relationship of spliced bars was approximately estimated equal to the fixed-end slip at the column-footing interface.

Local Bond Stress-Slip Relationship

Fig. 11 presents the local bond stress-slip envelope curves of the spliced bars for both directions of loading. At the ascending branch, the τ-s relation is linear for all tested specimens up to peak bond stress, while at the postpeak branch, the shape of the curves between confined and unretrofitted columns is diversified. The splitting of the concrete cover along the weak plane formed by the lapped bars resulted in a sudden loss of the bond resistance, for both unretrofitted columns [Figs. 11(a) and 11(c)]. The mean value (in both directions of loading) of slip at conventional failure of specimens L20d_C and L40d_C was 4.6 mm and 6.6 mm, respectively.

The postpeak response of FRP and TRM confined columns was far better. Confinement of concrete in the column lap splice region by FRP and TRM jackets improved the bond resistance of spliced

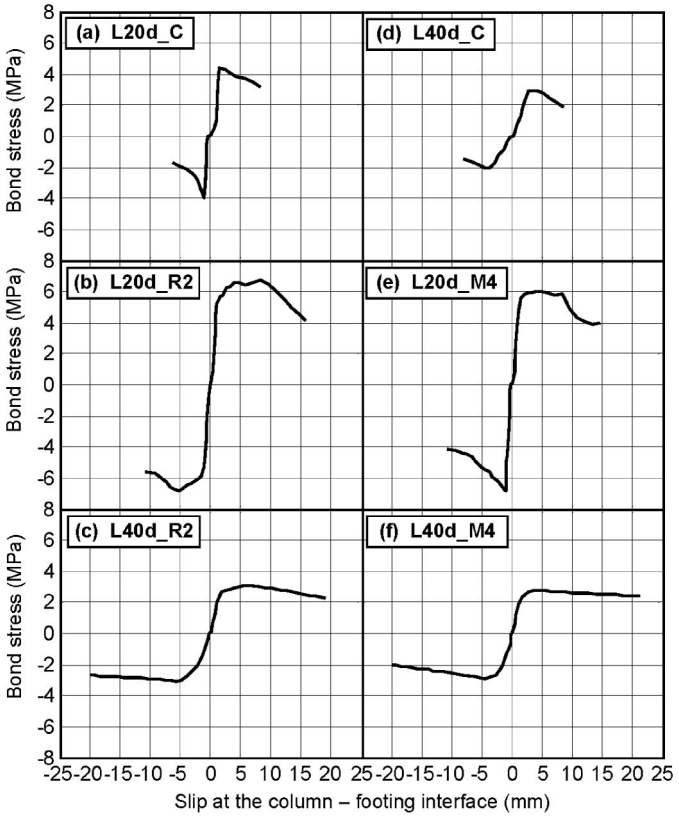

Fig. 11. Local bond-slip relationship for retrofitted and unretrofitted specimens: (a), (b), and (c) short lap splices; (d), (e), and (f) long lap splices

bars and resulted in a more ductile and stable behavior. More specifically, for specimens L20d_R2 and L20d_M4, splitting of concrete was controlled and did not lead to direct degradation of bond stresses, since spalling of the cover was prevented by the jackets. Thus, high bond stresses were maintained approximately constant (in at least one direction of loading) for 4–6 loading cycles after peak bond stress. However, when the longitudinal splitting cracks propagated over the entire splice length, splitting induced pull-out bond failure of the spliced bars. At that point, the presence of FRP or TRM jacket had no effect on the residual bond capacity of the bars, because the last were moving as a rigid body over the lap splice region, displaying a residual bond resistance because of friction mechanisms. This residual bond capacity results from the presence of external composite jackets, which maintain concrete integrity and provide quite significant mechanical interaction with the corner bars. The mean value (in both directions of loading) of slip at conventional failure of specimens L20d_R2 and L20d_M4 was 12.1 mm and 8.8 mm, respectively.

On the contrary, in specimens L40d_R2 and L40d_M4 the calculated bond stresses were measured approximately equal to the concrete's tensile strength, 3.1 MPa and 2.9 MPa, respectively. As a consequence, longitudinal splitting cracks did not propagate over the entire lap length and spalling of the concrete was suppressed until the end of the test at a drift ratio of 7.81%. Hence, bond stresses were maintained constant until the test was terminated, resulting in a nearly elastic, perfectly plastic τ-s relationship.

Conclusions

In the present study, the mechanism by which confinement with composite jackets (FRP and TRM) contributes to the enhancement

of the bond resistance between lap-spliced bars and concrete was investigated experimentally and analytically. The evolution of bond stresses at the critical regions of full-scale columns subjected to seismic loading, based on direct strain gauge measurements on the lap-spliced bars, magnifies the validity of the relatively limited number of the six tested specimens. Contrary to pull-out bond tests, the test setup selected in this study reproduces realistically the bond conditions between lap-spliced bars and concrete at the plastic hinge region of columns subjected to seismic loading. More specific conclusions are summarized in a rather qualitative manner as follows:

- The short lap splice length of 20 bar diameters is deficient for the development of longitudinal bars yield strength, while the longer lap length of 40 bar diameters was found to be sufficient for the development of bars' yield stress in one loading direction only. Moreover, for both unconfined specimens, splitting of the concrete cover at the lap splice region led to the sudden drop of the load resistance and to the decrease of columns' deformation capacity. The bond strengths measured experimentally for both unconfined specimens with short and long lap lengths were found in good agreement with the models of Zuo and Darwin (2000) and Lettow and Eligehausen (2006), respectively.
- Both FRP and TRM jackets resisted the propagation of longitudinal splitting cracks, resulting in the increase of the bond strength between lap-spliced bars and concrete. In general, the external confinement with composite jackets and the enhancement of the local bond-slip relationship along the lap-splice region resulted in the enhancement of the global response of the confined columns both in terms of strength and deformation capacity at failure.
- The contribution of FRP or TRM confinement on the local bond strength of lap splices is taken into account by proper modifications of the two aforementioned bond models. The proposed parameter for the modification takes into account all the characteristics of the jacket: the area of external FRP or TRM reinforcement in the splice region, the effect of the modulus of elasticity of the jacket's composite material, and the average effective strain of the jacket in the circumferential direction.
- For short lap splices, the composite jacket's part that extends outside the lap splice region is activated more, as compared with longer lap splices, since it resists more and in a more extended zone against the propagation of longitudinal splitting cracks.
- The average effective strain in which the composite jacket is activated in the lateral direction decreases as the ratio ℓ_s/d_b increases. Hence, a rational design of the jacket thickness, to provide that steel yielding will precede bond failure of the rebar, is possible if one incorporates the dependence of the transverse jacket strains on the ratio ℓ_s/d_b. The most reliable approach for doing so is shown in Eqs. (9*c*) and (9*d*).
- The slip for the calculation of the local bond stress-slip constitutive law of spliced bars was approximately equal to the fixed-end slip at the column-footing interface. Reduction of the fixed-end slip cannot be achieved through confinement at joint regions because the fixed-end slip at the base crack is a function of the horizontal displacement and thus it is not possible to control this slip through jacketing.

Despite their relatively limited number, all test results presented in this study indicate that confinement with composite jackets is an extremely promising solution with great potential for the enhancement of the local bond behavior between lap-spliced bars and surrounding concrete. Future research should be directed toward providing a better understanding of parameters including different ℓ_s/d_b ratios; the bond stress distribution over and outside the lap length; the stiffness of the jacket in the circumferential direction; the height of the jacket to lap splice length of the bars h_f/ℓ_s; and the value of the parameter $K_{tr,j}$ beyond which bond failure is not controlled by splitting but by bar pull-out.

Acknowledgments

The writers wish to thank Lecturer C. Papanicolaou for her assistance in the experimental program. The work reported in this paper was funded by the Greek General Secretariat for Research and Technology through the project ARISTION, within the framework of the Built Environment and Management of Seismic Risk program.

Notation

The following symbols are used in this paper:

A_b = area of longitudinal bars;
A_{sw} = area of transverse steel reinforcement parallel to the direction x within s_h;
$c_{\max}$, $c_{\min}$ = maximum, minimum concrete cover;
d_b = diameter of lapped bars;
E_f = elastic modulus of jacket in the lateral direction;
E_s = elastic modulus of steel;
f_c = compressive strength of concrete;
f_{sL} = stress of longitudinal reinforcement;
f_{sm} = maximum stress in the tensile bars at lap splice regions at splitting bond failure;
f_{yL} = yield stress of longitudinal reinforcement;
f_{yw} = yield stress of stirrups;
h_f = height of the FRP or TRM jacket;
$K_{tr,j}$ = term representing the effect of confinement by FRP or TRM jackets;
$K_{tr,s}$ = term representing the effect of confinement by steel stirrups;
$K_{tr,t}$ = term representing the effect of total confinement;
k_f = calibration factor for the effectiveness of the FRP or TRM jacket;
k_s = calibration factor for steel transverse reinforcement;
ℓ_d, ℓ_{dy} = development lengths of elastic and plastic region of bars in the anchorage;
ℓ_i = distance of cross section i from the column base, $i = 1, 2, 3$;
ℓ_s = lap length;
M = moment at end section;
M_y = yield moment of cross section;
N = number of transverse reinforcing bars (stirrups or ties) crossing ℓ_s;
n = number of layers of the fiber sheet or textile;
$n_{l,sw}$ = number of transverse reinforcing bars (stirrups or ties) crossing splitting cracks;
n_s = number of transverse reinforcing bars spliced along the plane of splitting;
R_r = ratio of projected rib area normal to bar axis to product of nominal bar perimeter and center-to-center rib spacing;
s_d = slip attributable to yield penetration of longitudinal bars in the anchorage region;
s_{el} = slip attributable to the spliced bars' elongation over the lap splice region;
s_h = spacing of stirrups;
t_d = $0.78d_{bL} + 5.6$, term representing effect of bar size (mm);
t_f = thickness of one fiber sheet or textile layer;

t_r = $9.6R_r + 0.28$, term representing the effect of relative rib area;
w_c = crack width at the column-footing interface;
x = direction of loading or coordinate along the splice length in Fig. 5(a);
α = angle of ribs in reinforcing bars;
$\Delta\ell_i$ = elongation of displacement transducer at section i, $i = 1, 2$
$\varepsilon_{\text{flex}}$ = mean strain in the extreme tension fiber at the column base;
$\varepsilon_{f,ef}$ = average effective strain of the jacket in the circumferential direction;
ε_i = axial strain of starter and longitudinal bars at discrete locations of strain gauges i, $i = 1, 2, 3$;
ε_{sw} = average effective strain of the stirrups in the circumferential direction;
τ = bond stress;
τ_{av} = average bond strength; and
$\tau_{\max}$ = bond strength between lap-spliced bars and concrete.

References

ACI Committee 408. (2003). "Bond and development of straight reinforcing bars in tension." *ACI 408R-03*, American Concrete Institute (ACI), Farmington Hills, MI, 49.

Azizinamini, A., Pavel, R., Hatfield, E., and Ghosh, S. K. (1999). "Behavior of lap-spliced reinforcing bars embedded in high-strength concrete." *ACI Struct. J.*, 96(5), 826–835.

Bournas, D. A., Lontou, P. V., Papanicolaou, C. G., and Triantafillou, T. C. (2007). "Textile-reinforced mortar (TRM) versus FRP confinement in reinforced concrete columns." *ACI Struct. J.*, 104(6), 740–748.

Bournas, D. A., Triantafillou, T. C., Zygouris, K., and Stavropoulos, F. (2009). "Textile-reinforced mortar (TRM) versus FRP jacketing in seismic retrofitting of RC columns with continuous or lap-spliced deformed bars." *J. Compos. Constr.*, 13(5), 360–371.

Bousias, S. N., Spathis, A.-L., and Fardis, M. N. (2007). "Seismic retrofitting of columns with lap-spliced smooth bars through FRP or concrete jackets." *J. Earthquake Eng.*, 11(5), 653–674.

Brena, S. F., and Schlick, B. M. (2006). "Hysteretic behavior of bridge columns with FRP-jacketed lap splices designed for moderate ductility enhancement." *J. Compos. Constr.*, 11(6), 565–574.

Cairns, J., and Arthur, P. D. (1979), "Strength of lapped splices in reinforced concrete columns." *ACI Struct. J.*, 762, 277–296.

Chang, K. C., Lin, K. Y., and Cheng, S. B. (2001). "Seismic retrofit study of RC rectangular bridge columns lap—spliced at the plastic hinge zone." *Proc., Int. Conf. of FRP composites in Civil Engineering*, Hong Kong, 869–875.

ElGawady, M., Endeshaw, M., McLean, D., and Sack, R. (2010). "Retrofitting of rectangular columns with deficient lap splices." *J. Compos. Constr.*, 14(1), 22–35.

EN 1015-11. (1993), *Methods of test for mortar for masonry, Part 11: Determination of flexural and compressive strength of hardened mortar*, European Committee for Standardization, Brussels, Belgium.

Federation internationale du Beton (fib). (2000). *Bond of reinforcement in concrete*, Bulletin 10, International Federation for Structural Concrete, Lausanne, Switzerland.

Hamad, B. S., and Rteil, A. A. (2006). "Comparison of roles of FRP sheets, stirrups, and steel fibers in confining bond critical regions." *J. Compos. Constr.*, 10(4), 330–336.

Harajli, M. H. (2005). "Behavior of gravity load-designed rectangular concrete columns confined with fiber reinforced polymer sheets," *J. Compos. Constr.*, 9(1), 4–14.

Harajli, M. H., and Dagher, F. (2008). "Seismic strengthening of bond-critical regions in rectangular reinforced concrete columns using fiber-reinforced polymer wraps." *ACI Struct. J.*, 105(1), 68–77.

Harajli, M. H., and Rteil, A. A. (2004). "Effect of confinement using fiber-reinforced polymer or fiber-reinforced concrete on seismic performance of gravity load-designed columns." *ACI Struct. J.*, 101(1), 47–56.

Haroun, M. A., Feng, M. Q., Bhatia, H., Baird, K., and Elsanadedy, H. M. (1999). "Structural qualification testing of composite—jacketed circular and rectangular bridge columns." *Final Report, California Department of Transportation*, Dept. of Civil and Environmental Engineering, Univ. of California at Irvine, Irvine, CA.

Haroun, M. A., Mosallam, A. S., Feng, M. Q., and Elsanedeby, L. L. (2001). "Experimental investigation of seismic repair and retrofit of bridge columns by composite jackets." *Proceedings of the International Conference of FRP composites in Civil Engineering*, J.-G. Teng, ed., Hong Kong, 839–848.

Harries, K. A., Ricles, J. R., Pessiki, S., and Sause, R. (2006). "Seismic retrofit of lap splices in nonductile square columns using carbon fiber-reinforced jackets." *ACI Struct. J.*, 103(6), 874–884.

Lettow, S., and Eligehausen, R. (2006). "Formulation of application rules for lap splices in the new model code." Presentation, Task group 4.5, Bond models, Stuttgart, Germany, Nov. 13, 2006.

Lukose, N., Gergely, P., and White, R. N. (1982). "Behavior of reinforced concrete lapped splices for inelastic cyclic loading." *ACI Struct. J.*, 79(5), 355–365.

Ma, R., and Xiao, Y. (1999). "Seismic retrofit and repair of circular bridge columns with advanced composite materials." *Earthquake Spectra*, 15(4), 747–764.

Ma, P., Xiao, Y., and Li, K. N. (2000). "Full-scale testing of a parking structure column retrofitted with carbon-fiber reinforced composites." *Constr. Build. Mater.*, 14(2), 63–71.

Melek, M., and Wallace, J. W. (2004). "Cyclic behavior of columns with short lap splices." *ACI Struct. J.*, 101(6), 802–811.

Orangun, C. O., Jirsa, J. O., and Breen, J. E. (1977). "Reevaluation of test data on development length and splices." *J. Am. Concr. Inst.*, 74(3), 114–122.

Osada, K., Yamaguchi, T., and Ikeda, S. (1999). "Seismic performance and the retrofit of hollow circular reinforced concrete piers having reinforcement cut-off planes and variable wall thickness." *Trans. Japan Concr. Inst.*, 21, 263–274.

Panahshahi, N., White, R. N., and Gergely, P. (1992). "Reinforced concrete compression lap splices under inelastic cyclic loading." *ACI Struct. J.*, 89(2), 164–175.

Paulay, T. (1982). "Lapped splices in earthquake-resisting columns," *ACI Struct. J.*, 79(6), 458–469.

Saadatmanesh, H., Ehsani, M. R., and Jin, L. (1997a). "Repair of earthquake-damaged RC columns with FRP wraps." *ACI Struct. J.*, 94(2), 206–215.

Saadatmanesh, H., Ehsani, M. R., and Jin, L. (1997b). "Seismic retrofitting of rectangular bridge columns with composite straps." *Earthquake Spectra*, 13(2), 281–304.

Saatcioglu, M., and Elnabelsy, G. (2001). "Seismic retrofit of bridge columns with CFRP jackets." *Proc., Int. Conf. of FRP Composites in Civil Engineering*, Hong Kong, 833–838.

Seible, F., Priestley, M. J. N., Hegemier, G. A., and Innamorato, D. (1997). "Seismic RETROFIT of RC columns with continuous carbon fiber jackets." *J. Compos. Constr.*, 1(2), 52–62.

Sezen, H., and Moehle, J. P. (2003). "Bond-slip behavior of reinforced concrete members." *Proc., FIB symposium, concrete structures in seismic regions*, Athens, Greece, May 2003.

Triantafillou, T. C., and Papanicolaou, C. G. (2006). "Shear strengthening of RC members with textile reinforced mortar (TRM) jackets." *Mater. Struct.*, 39(1), 85–93.

Triantafillou, T. C., Papanicolaou, C. G., Zissimopoulos, P., and Laourdekis, T. (2006), "Concrete confinement with textile-reinforced mortar jackets." *ACI Struct. J.*, 103(1), 28–37.

Valluvan, R., Kreger, M. E., and Jirsa, J. O. (1993). "Strengthening of column splices for seismic retrofit of nonductile reinforced concrete frames." *ACI Struct. J.*, 91(46), 432–440.

Zuo, J., and Darwin, D. (2000). "Splice strength of conventional and high relative rib area bars in normal and high-strength concrete." *ACI Struct. J.*, 97(4), 630–641.